The 11th Canadian Conference on Earthquake Engineering
Canadian Association for Earthquake Engineering
11CCEE

GFRP-RC COLUMNS UNDER REVERSAL CYCLIC LOADING

Mahmoud Ali
M.Sc. Student, Dept. of Civil Eng., University of Manitoba, Winnipeg, MB, Canada
mohamed5@myumanitoba.ca

Ehab El-Salakawy
Professor and CRC, Dept. of Civil Eng., University of Manitoba, Winnipeg, MB, Canada
Ehab.El-Salakawy@umanitoba.ca

ABSTRACT: The non-corrodible fiber-reinforced polymer (FRP) bars have emerged as an attractive alternative to steel reinforcement in engineering applications, where surviving extreme weathering conditions and/or the application of de-icing salts is a concern. Compared to steel reinforcement, FRP bars have linear-elastic behaviour with relatively low modulus of elasticity, which raised concerns on the feasibility of replacing the inelastic behaviour of steel reinforcement in earthquake-resistant structures. This paper presents experimental data on the seismic performance of rectangular columns reinforced internally with glass (G) FRP longitudinal and transverse reinforcement. Five full-scale GFRP-reinforced concrete (RC) columns, with 1650-mm shear span and 350-mm square cross-section, were constructed and tested under constant axial compression and incrementally increasing lateral load reversal. The geometry of the test prototypes was selected to simulate the lower portion of first storey columns between the footing and the contra-flexure point. The test variables presented in this paper include longitudinal reinforcement ratio and degree of confinement. The test results showed that reducing the vertical spacing between the transverse reinforcement improved the deformability with insignificant strength degradation before failure, while increasing the reinforcement ratio resulted in higher strength gain with lower drift capacity at failure.

1. Introduction

Considering the catastrophic effect of earthquakes on the social life as well as the economy, rapid development of materials, design, and construction techniques have been always required. Unfortunately, steel-RC structures are vulnerable to corrosion of steel reinforcement, which can lead to loss of serviceability, reduction of load carrying capacity, and even partial or full collapse. Therefore, one of the serious attempts for alternative materials to the ordinary steel is the non-corrodible glass fibre-reinforced polymers (GFRP). However, the application of GFRP bars in earthquake-resistant structures yet to be verified due to their different mechanical and bond characteristics compared to steel. GFRP reinforcement exhibits linear elastic behaviour up to failure with low modulus of elasticity. These characteristics produce deformable structural members under reversed-cyclic loading, which may replace the inelastic behaviour (ductility) of steel reinforcement in dissipating the seismic energy in earthquakes-resistant columns.

To date, very limited research has been conducted to investigate the seismic performance of GFRP-RC columns. Sharbatdar et al. (2004) reported that columns reinforced internally with Carbon (C) FRP longitudinal bars and grids can be design to satisfy strength and deformability requirements of earthquake resistant structures. Tavassoli et al. (2015) concluded that columns reinforced with GFRP bars and spirals showed stable behaviour up to failure. Furthermore, the GFRP spirals delayed crushing of the concrete core, which increased the deformability of the columns.

2. The Experimental Program

2.1. Test prototypes

This paper reports part of an on-going experimental program in the McQuade Heavy Structures Laboratory at the University of Manitoba, in which full-scale square columns are constructed and tested under simultaneous constant axial load and simulated seismic loading. The test specimens simulate the lower portion of first storey columns between the footing and the contra-flexure point. As shown in Figure 1, the test specimens had a 350-mm square cross-section and a shear span of 1650-mm (distance between the footing and point of load application). These dimensions were chosen to promote flexure failure in addition to be representative of the columns commonly found in concrete structures.

The test results and discussion for five specimens are presented in this paper. The test prototypes were reinforced internally with GFRP longitudinal and transverse reinforcement. The Canadian standards CSA S806-12 (CSA 2012) was used to design the test specimens. A constant axial load of 0.1 $f'_c A_c$ was applied to all columns during the entire test. Column G-C with 1.3% reinforcement ratio and 75-mm stirrup spacing, was used as a control specimen. Columns G-S-100 and G-S-150 had a stirrup spacing of 100, 150 mm, respectively, in order to provide different degree of confinement, while columns G-R-1.9, and G-R-2.6 with 1.9 and 2.6% reinforcement ratio, respectively, were used to study the reinforcement ratio parameter.

Table 1 – Characteristics of test specimens

Specimens	Reinforcement ratio, ρ (%)	Longitudinal Bars	Stirrups
G-C-1.3	1.3%	8 No.16	No.10@75 mm
G-R-2.6	2.6%	16 No.16	
G-R-1.9	1.9%	12 No.16	
G-S-100	1.3%	8 No.16	No.10@100 mm
G-S-150			No.10@150 mm

2.2. Materials

All test prototypes were cast and wet-cured in the laboratory for 7 days. Normal-weight, ready-mixed concrete with a specified 28-day compressive strength of 35 MPa was used. The maximum nominal aggregate size was 19 mm, and the measured slump of the concrete was 120 mm. The average concrete compressive strength was approximately 38.5 MPa on the day of testing based on standard cylinder tests (152×305 mm). Sand-coated GFRP bars were used in this study (Pultrall Inc. 2012). The properties of the reinforcement as provided by the manufacturer are listed in Table 2.

Table 2 – Properties of reinforcing bars

Bar Type	Bar diameter (mm)	Bar area (mm^2)	Modulus of elasticity (GPa)	Tensile strength (MPa)	Ultimate strain (%)
No.16	15.9	198	62	1184	1.89
No.10 [a]	9.5	71	52	1022	1.97

[a] Properties of the straight portion of the bent GFRP bar.

2.3. Test setup and loading scheme

As shown in Figure 1, the simulated seismic load was applied using a 1000-kN fully dynamic actuator of ±250-mm stroke. In addition, a hinged-loading frame was used to transfer the axial load from a 1000-kN capacity hydraulic jack to the column specimen while allowing the column to translate laterally. In order to simulate the rational fixity of the first storey column; a heavily reinforced footing was fixed to the strong floor.

To simulate the seismic loading in the laboratory, a load scheme consisted of a load-controlled phase followed by a displacement-controlled phase was applied to all test specimens. During the load-controlled phase, two load cycles were applied. The first cycle was to reach the cracking load; while the second cycle represented the service loading condition for the GFRP bars (25% of the ultimate tensile strength of the GFRP longitudinal bars (CSA 2012)).

On the other hand, the displacement-controlled phase was carried out according to the recommendations of the ACI Committee 374 Report (ACI 374.1 2005). In this phase, the load was applied at quasi-static rate of 0.01 HZ. Figure 2 shows the loading scheme, the numbers on top are the drift ratios (y-axis values), while the numbers on the X- axis are the cycle numbers.

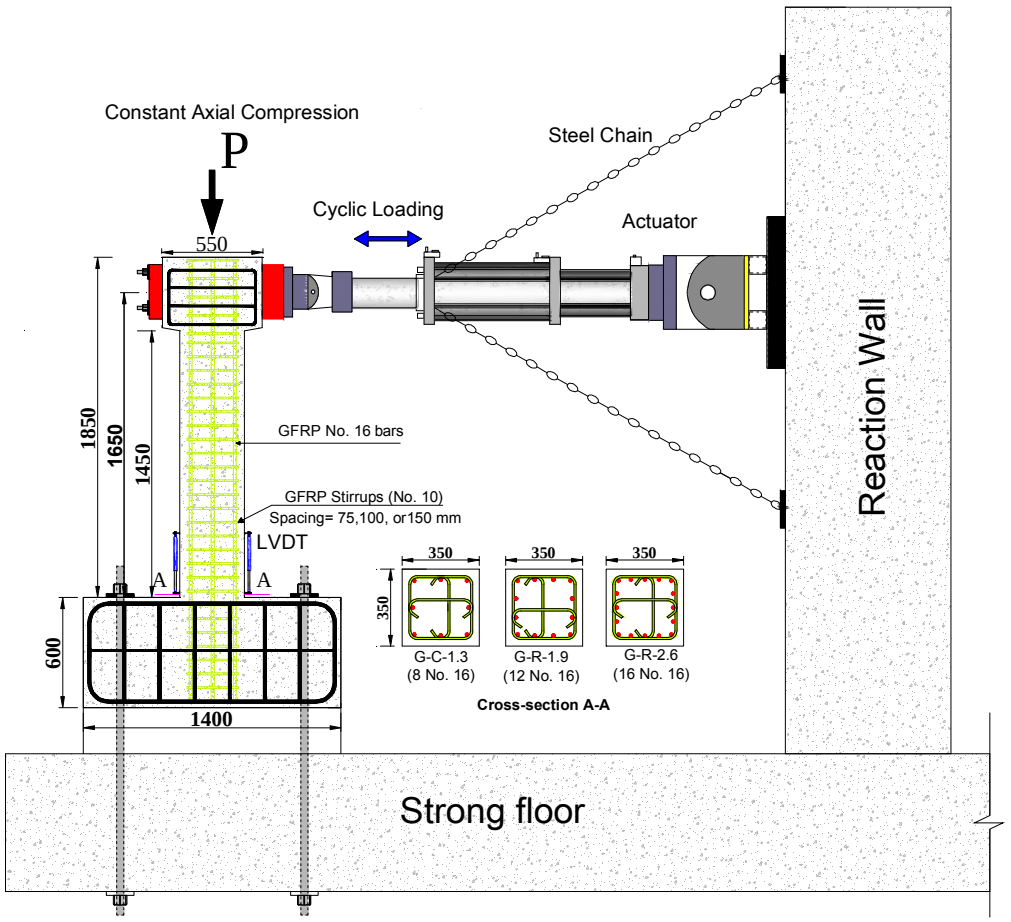

Fig. 1 – Test set-up

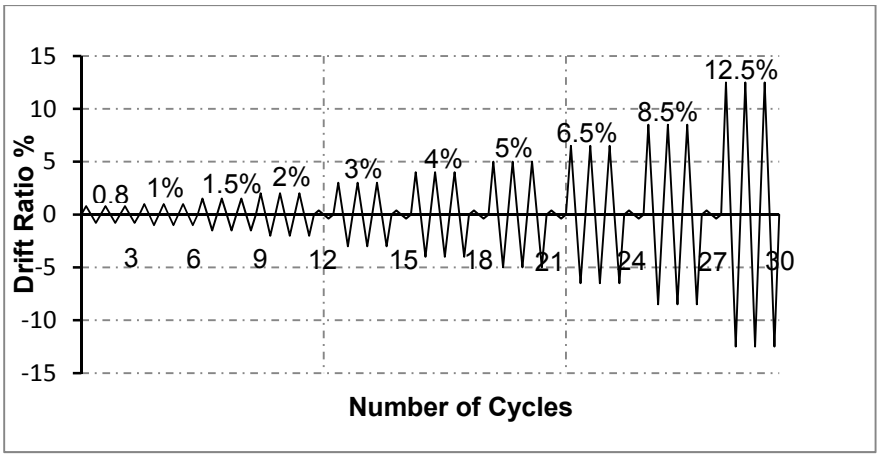

Fig. 2 – Seismic loading scheme

3. Test Results and Discussion

3.1. Crack pattern and mode of failure

The general observation for all test specimens during testing indicated that many flexure cracks were developed upon the application of the displacement loading cycles. In addition, a continuous crack was initiated at the column-footing interface due to the significant elastic deformation of the longitudinal bars at the footing surface. As the loading continued, more cracks were observed while the existing cracks were getting wider with propagation into the column side faces. The intensity of cracks was uniformly distributed on the lower half of the column when the concrete cover started to spall off at 3% drift ratio. At the subsequent loading cycles, spalling of the concrete cover was limited to the hinging region in most specimens. Only specimen G-C-1.3 had spalling of the concrete cover from the footing-column interface up to approximately the mid-height of the column at failure.

Flexure failure was observed in all specimens. Failure typically occurred by crushing of concrete followed by a compression failure of the longitudinal bars. Only specimens G-S-100 and G-S-150 showed both buckling and compression failure due to the larger stirrup spacing. It is worth mentioning that specimen G-C-1.3 failed at the first cycle of 12.5% drift ratio, while the rest of the specimens failed at 8.5% drift ratio. This behaviour showed an agreement with the previous experimental work conducted on circular GFRP-RC columns by Tavassoli et al. (2015), when columns with smaller spiral spacing and adequate longitudinal reinforcement ratio showed enhancement in the deformability at failure. Figure 3 shows photos of the test specimens at failure.

3.2. Hysteresis Behaviour

The hysteric diagram represents the relationship between the applied lateral load and the drift ratio of the column tip. The drift ratio was calculated as the horizontal displacement of the column divided by the unsupported height of the column. As shown in Figure 4, the hysteresis diagrams of all the test specimens showed similar behaviour during loading (the ascending portion of the hysteresis diagram) and unloading stages (descending portion of the hysteresis diagram). During loading at the early stages, all the test specimens showed linear behaviour due to the elastic behaviour of the GFRP reinforcement. However, specimens G-S-100 and G-S-150 showed non-linear behaviour of the lateral load-drift ratio relationship envelop after 3% drift ratio. This behaviour was attributed to the non-linear behaviour of the concrete after spalling of the concrete cover due to lower confinement of the larger spacing between stirrups. On the other hand, during unloading, the hysteresis diagram for all the specimens aimed approximately at the origin of the lateral load-drift ratio relationship, which explains the insignificant residual deformation due to pinching.

(a) G-C-1.3

(b) G-S-100

(c) G-S-150

(d) G-R-1.9

(e) G-R-2.6

Fig. 3 – Mode of failure of the tested specimens

Previous research on circular GFRP-RC columns under seismic loading (Tavassoli et al. 2015) has shown that decreasing the spacing of spiral reinforcement developed higher strength and deformability. Similar behaviour was obtained in the current study. Specimens with smaller stirrup spacing showed enhanced deformability in addition to higher strength gain, while specimens with higher reinforcement ratio showed higher lateral resistance with lower drift capacity at failure. For example, specimen G-C-1.3 has reached up to 12.5% drift ratio with insignificant strength degradation at failure. Failure for specimens G-S-150 and G-S-100 occurred at first and second cycle of 8.5% drift ratio, respectively, however, there was insignificant increase in the lateral capacity after 3% drift ratio. For specimens G-R-2.6 and G-R-1.9, failure occurred at first and third cycle of 8.5% drift ratio, respectively, with approximately up to 20% increase in the lateral load resistance compared to the control specimen (G-C-1.3) at failure.

3.3. Energy Absorption

Figure 5 shows the cumulative energy dissipation of the test specimens. The cumulative energy dissipation was calculated by the total area enclosed in completed hysteresis loops at each loading step. Similar to the test results of the circular GFRP-RC columns under seismic loading (Tavassoli et al. 2015), all test specimens showed approximately the same level of absorbed energy at 4% drift ratio. For example, at 4% drift ratio, the absorbed energy for all specimens ranged between 19 and 22%. This is in good agreement with the similar hysteresis response of the test specimens, as discussed earlier. It is worth mentioning that only specimen G-C-1.3 showed approximately 60% increase in the cumulative energy absorbed at failure due to higher drift capacity.

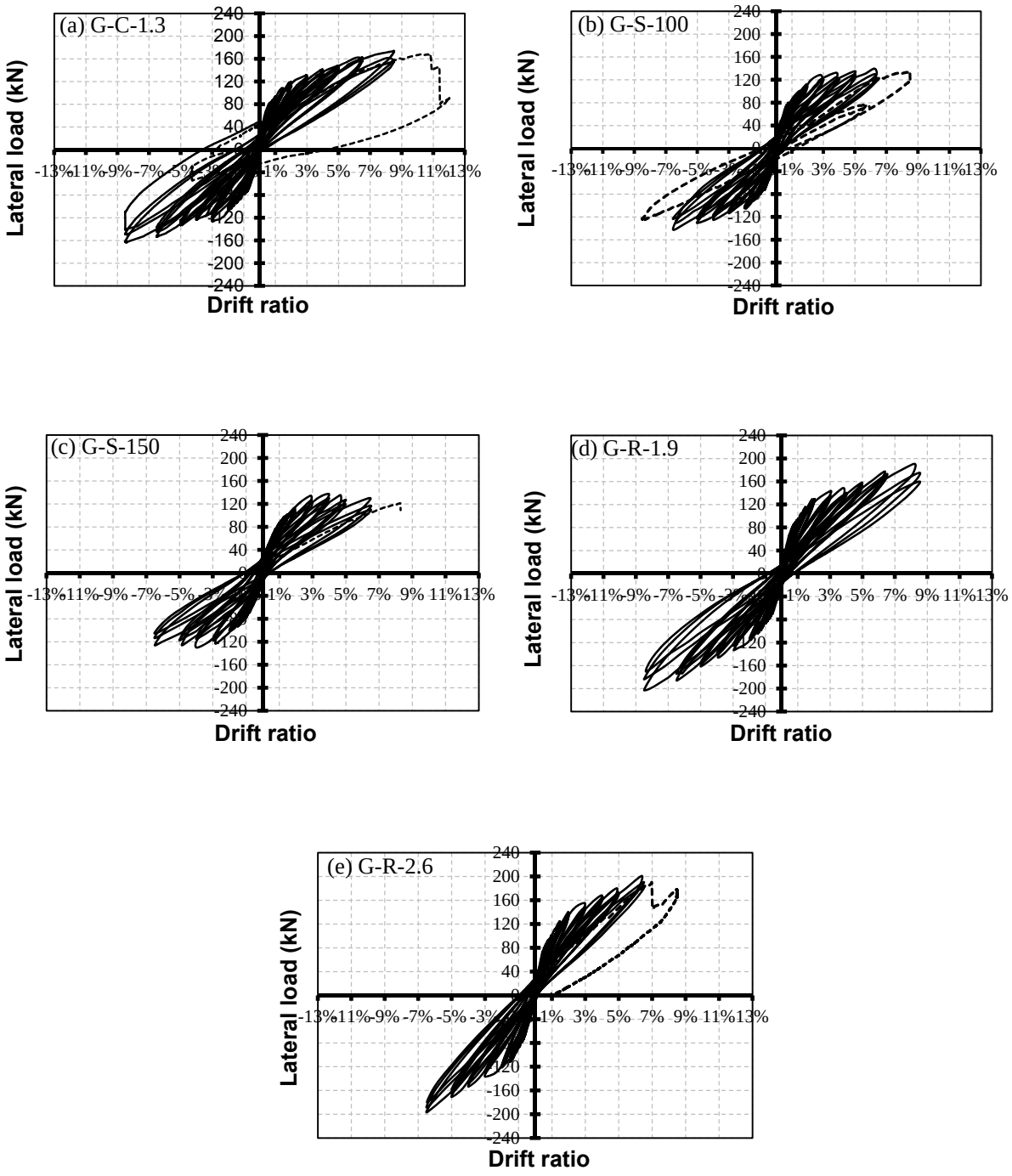

Fig. 4 – Hysteretic load-drift ratio relationship

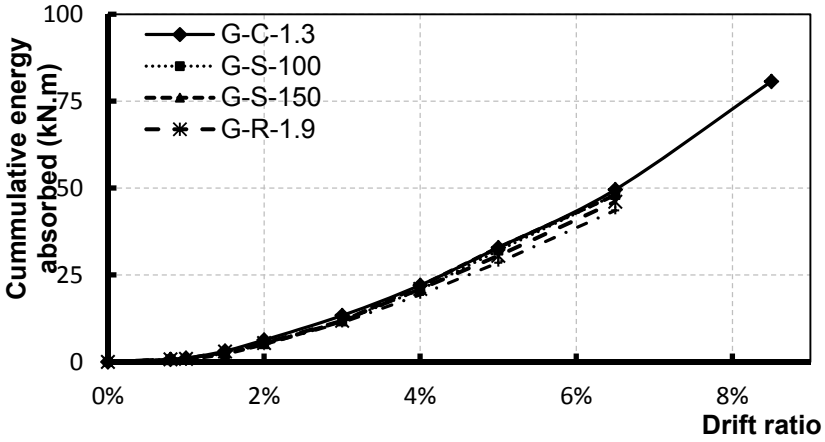

Fig. 5 – Cumulative energy absorbed by test specimens

4. Conclusions

Based on the experimental results, the following conclusions are drawn.

1. The GFRP-RC columns showed stable behaviour when sustaining gravity load in the presence of the reversed-cyclic loading. Furthermore, the drift capacity of all the test specimens was more than the 2.5% and the 4% required by the National Building Code of Canada (NRCC 2010) and CSA/S806-12 (CSA 2012), respectively.
2. Reducing the spacing between stirrups improved the deformability as well as the strength gain of the columns. For example, compared to specimen G-S-100 and G-S-150, specimen G-C-1.3 reached 200% increase in the drift capacity with 25% increase in the strength gain.
3. Increasing the reinforcement ratio showed higher lateral load resistance with lower drift capacity at failure. For example, specimen G-R-1.9 and G-R-2.6 showed approximately 50% decrease in the drift capacity with 20% strength gain compared to the control specimen (G-C-1.3).
4. All test specimens showed approximately the same level of the absorbed energy at each loading step due to the elastic behaviour of the GFRP reinforcement. For example, at 4% drift ratio, all test specimens reached approximately the same level of the cumulative energy absorption (22 kN.m). However, specimen G-C-1.3 reached 80 kN.m at failure due to higher drift capacity.

5. Acknowledgements

The authors wish to express their gratitude and sincere appreciation for the financial support received from the Natural Science and Engineering Research Council of Canada, through Canada Research Chairs program and the Network of Centers of Excellence on Intelligent Sensing for Innovative Structures (ISIS Canada). The help received from the technical staff of the McQuade Heavy Structures Laboratory at the University of Manitoba is also acknowledged.

6. References

ACI Committee 374. “Acceptance criteria for moment frames based on structural testing and commentary.” ACI 374.1-05, American Concrete Institute, Farmington Hills, Detroit, 2005, 9 p.

Canadian Standards Association (CSA). “Design of concrete structures.” CSA/A23.3-04, Canadian Standards Association, Rexdale, Ontario, 2004, 214 p.

Canadian Standards Association (CSA). “Design and construction of building components with fibre-reinforced polymers.” CSA/S806-12, Canadian Standards Association, Rexdale, Ontario, 2012, 177 p.

National Research Council of Canada (NRCC). “National Building Code of Canada (NBCC).” National Research Council of Canada, Ottawa, Ontario, 2010, 1167 p.

Pultrall Inc. (2012). “V-ROD^{TM}, Technical Data Sheet”. ADS Composites Group Inc. http://www.pultrall.com, Thetford Mines, Quebec, Canada.

Sharbatdar, M. K. and Saatcioglu, M. “Behavior of FRP reinforced concrete under cyclic loading.” 13^{th} *Int. Conf. on Earthquake Engineering, (WCEE-04*), Vancouver, British Columbia, August 2004.

Tavassoli, A., Liu, J. and Sheikh, S. “Glass fiber-reinforced polymer-reinforced circular columns under simulated seismic loads.” *ACI Structural Journal*, Vol. 112, No.10, January 2015, pp.103-114.